Original Article

Comparison of micro-CT image enhancement after use of different vascular casting agents

Ryan Margolis[1], Brian Merlo[1], Dara Chanthavisay[1], Chastity Chavez[1], Brian Trinh[1], Junjie Li[1,2]

[1]Department of Bioengineering, University of Texas at Dallas, Richardson, TX, USA; [2]Department of Surgery, Beth Israel Deaconess Medical Center, Harvard Medical School, Boston, MA, USA

Contributions: (I) Conception and design: R Margolis, J Li; (II) Administration support: J Li; (III) Provision of study materials or patients: J Li; (IV) Collection and assembly of data: R Margolis, B Merlo, J Li, D Chanthavisay, B Trinh, C Chavez; (V) Data analysis and interpretation: R Margolis, B Merlo, D Chanthavisay, C Chavez; (VI) Manuscript writing: All authors; (VII) Final approval of manuscript: All authors.

Correspondence to: Junjie Li, PhD. Department of Bioengineering, University of Texas at Dallas, Richardson, TX, USA; Department of Surgery, Beth Israel Deaconess Medical Center, Harvard Medical School, 330 Brookline Avenue, Boston, MA 02215, USA. Email: jli37@bidmc.harvard.edu.

Background: Microvascular visualization is crucial in understanding the mechanisms of several pathologies. For instance, visualization of the tumor microenvironment is important in understanding angiogenesis and role in cancer progression. Visualization would provide insights to cancer diagnosis, predicting metastatic growth, and evaluating therapeutic protocols. Similarly, understanding the microvascular network could be beneficial for study of degenerative diseases and tissue repair. The use of microscale computed tomography (micro-CT) and vascular casting agents provides high-resolution images of tissue vasculature in volumetric space. The purpose of this research was to compare a selection of commercially available contrast agents to determine the optimal solution for vascular visualization.

Methods: A population of 16 female nude athymic mice (Charles Rivers Laboratories) were implanted with MDA-MB-231 breast cancer cells (ATCC) orthotopically in the lower left mammary fat pad to investigate the tumor microenvironment. Once tumors reach sufficient size, animals were equally divided into four groups based on the micro-CT agent to be administered, namely, control (no contrast agent), barium sulfate ($BaSO_4$), Vascupaint, or Microfil. Animals were anesthetized prior to transcarotid micro-cannulation to infuse 2 mL of the specific contrast agent for intravascular distribution throughout the animal. The jugular vein on the other side of the carotid artery was opened to drain blood flow. Following successful perfusion, animals and extracted organs underwent high-resolution micro-CT scanning (OI/CT, MILabs). Images were reconstructed and analyzed using analysis software to extract mean intensity signals.

Results: Preliminary post-mortem micro-CT results reveal Vascupaint and $BaSO_4$ are useful for microvascular visualization. Both Vascupaint and $BaSO_4$ produced significant contrast-enhanced micro-CT image enhancement in the brain (3.39±0.93 and 6.27±3.78, respectively) and kidney (12.85±1.98 and 32.87±10.03, respectively) as compared to Microfil (0.22±0.07 and 0.91±0.63, respectively; $P<0.05$). For the various contrast agents, there were no differences in image enhancement from the liver, spleen, or tumor tissue ($P>0.21$). Moreover, use of Vascupaint and $BaSO_4$ allowed for visualization of smaller microvascular structures with average diameters of 20.54±4.15 and 25.82±3.75 µm, which were smaller compared to the 91.66±24.91 µm measurements from Microfil-enhanced micro-CT images ($P<0.004$).

Conclusions: Our study suggests that the use of Vascupaint and $BaSO_4$ is more than sufficient for *ex vivo* visualization of microvascular structures with contrast-enhanced micro-CT imaging as these contrast agents more effectively perfused smaller blood vessels.

Keywords: Micro-computed tomography (micro-CT); vascular imaging; Microfil; barium sulfate ($BaSO_4$); Vascupaint

Submitted Jun 21, 2023. Accepted for publication Jan 10, 2024. Published online Mar 06, 2024.
doi: 10.21037/qims-23-901
View this article at: https://dx.doi.org/10.21037/qims-23-901

Introduction

The human vascular network provides pathways for the transport of oxygen and other nutrients to their intended organs while removing carbon dioxide and other wastes (1). These processes are sustained through the continual growth of new blood vessels through a process called angiogenesis (2,3). This complex hierarchical network of arteries, veins, and capillaries provides the foundation for our health. Any restrictions to these pathways can lead to the development of various diseases, such as neurological diseases (3), occlusive vascular disorders (4), or cancer (5). Therefore, visualization of the vasculature can provide insights into the underlying mechanisms behind the development of such diseases. In particular, the field of oncology can benefit greatly from this knowledge gap, as cancer is a global healthcare dilemma. It is estimated that more than 1.95 million people will be diagnosed in the United States in 2022 (6).

New cancer therapies are continually being developed to counteract the complexities of neoplastic disease to treat the primary tumor but also prevent metastatic growth. Tumor angiogenesis develops new vasculature from pre-existing vessels. However, tumor vasculature is chaotic and leaky due to the presence of large pores in the endothelial lining of the vessels and the absence of continuous pericyte and smooth muscle coverage (5). These abnormalities disrupt the transport of nutrients, but more importantly, therapeutics within the tumor microenvironment. Furthermore, tumor growth is correlated with the upregulation of growth factors and receptors, such as the vascular endothelial growth factor (VEGF) and its receptor (VEGFR-1), and are known to impact vascular permeability, proliferation, and metastatic growth (5). Understanding angiogenesis is crucial to understanding the mechanisms behind cancer progression as tumors demonstrate inter- and intratumor heterogeneity. This can be achieved by visualizing the vascular network within the tumor microenvironment, which is crucial for cancer diagnosis (7), predicting metastatic growth (8), and evaluating therapeutic efficacy and protocols (9). Similar benefits could be made from vascular visualization for other degenerative diseases, such as stroke (10). Furthermore, vascular visualization is required as a reference standard for super resolution imaging algorithms and other computer models to prove validity.

There is a major need for improved methods and techniques that enable visualization of vasculature. Confocal and two-phwoton microscopy have previously been used to image microvasculature (11). However, they lack the penetration depth required to observe the entire vascular architecture. This also holds true for histology, which is often the gold standard for quantifying microvasculature. Histological samples provide no information about the three-dimensional (3D) vascular architecture or patterns (4). In addition, shrinkage and tissue distortion during sample preparation can further complicate results. Thus, there is a need to study the entire vascular network in volumetric space. However, 3D microscopy, although better than the 2D method, still relies heavily on the spatial orientation of the vessel to extract measurements (11). This goal can be achieved using micro-computed tomography (micro-CT). The vascular network can be enhanced following an injection of longitudinal *in vivo* or vascular casting contrast agents. Micro-CT imaging in conjunction with *in vivo* contrast agents allows for high-resolution scans for temporal measurements. One commonly used contrast agent is iodine. While it improves the vascular visualization, these agents are rapidly cleared from the blood through renal filtration within a few minutes and often not homogeneous (12,13). However, other smaller nanoparticle sized *in vivo* contrast agents have a high propensity to extravasate through leaky vasculature into tissues as early as 24 h and last up to 5 d (5). Other *in vivo* contrast agents are known to have even higher retention rates. Fenestra LC (Advanced Research Technologies Inc., Montreal, Canada), Exitron nano 6000 (Viscover, Milteny Biotech, Bergisch-Gladbach, Germany), and Exitron nano 12000 (Viscover, Milteny Biotech) maintained strong concentrations to allow for liver and spleen imaging 29 d after a single bolus

injection (14). More importantly, these contrast agents were shown to have capillaries filled with aggregates (14) or air (15) surrounding major blood vessels, suggesting that the nanoparticle aggregates block the glomerular capillary loops located at the beginning of the capillary network (16). These issues can lead to an incomplete or misleading model of the vascular network.

To overcome deficiencies of *in vivo* contrast agents for complete microvascular network visualization using micro-CT imaging, vascular casting contrast agents are often used. These contrast agents are pigmented or radiopaque casting materials that are injected throughout the animal for vascular visualization *in situ*, often through transcardiac perfusion procedures (10). These materials are mixed with a curing agent that polymerizes the contrast agents, allowing for these agents to remain within vascular structures. It is important to note that the use of these vascular casting contrast agents result in terminal studies. One of the more commonly used commercial products is Microfil (Flow Tek Inc., Carver, MA, USA). However, due to the higher viscosity and non-miscible nature of this compound, higher pressures are required to achieve uniform vascular filling, resulting in vessel bulging or even rupture (10). Therefore, there is a need to explore other available contrast agents that can successfully perfuse the vasculature to create a complete intravascular model. In this study, we qualitatively and quantitatively compare a barium-based casting formulation and a new commercially available silicone rubber casting agent against the gold standard Microfil to determine the optimal contrast agent for arterial vascular visualization by high-resolution micro-CT imaging. Both these contrast agents have a higher radiopacity, lower viscosity, and shorter curing time (roughly 20–30 minutes) than Microfil. While visualization of the tumor microvasculature was our primary target for understanding future cancer therapeutics, other organs were imaged to determine the uniformity in perfusion across other frequently targeted regions, such as the brain, kidney, liver, and spleen. Although other organs, such as the heart and skin, could be visualized using this technique, they were not considered for this study. We hypothesize that the barium-based and silicone rubber casting agents will provide a more complete vascular network visualization than Microfil in all organs. We present this article in accordance with the ARRIVE reporting checklist (available at https://qims.amegroups.com/article/view/10.21037/qims-23-901/rc).

Methods

Cell lines and culture

The human breast cancer MDA-MB-231 cells were cultured in Dulbecco's Modified Eagle's Medium (ATCC, Manassas, VA, USA) supplemented with 10% fetal bovine serum (v/v) and 1% penicillin-streptomycin (v/v). Cells were maintained in 75 cm^2 culture flasks and placed in a humidified incubator (Heracell 150i, Thermo Fisher Scientific, Waltham, MA, USA) with 5% CO_2 and maintained at 37 ℃. The cultured cells were allowed to grow until passage 10 and were counted using a digital cell counter (Countess II Automated Cell Counter, Thermo Fisher Scientific).

Animal protocol

This study was approved by the institutional ethics committee of the University of Texas at Dallas in compliance with national guidelines for the care and use of animals (OLAW Assurance Number: A3329-01 and USDA License Number: 74-R-0066). The 6- to 8-week-old female athymic nude mice (N=16, Charles River Laboratories, Wilmington, MA, USA) were injected with 1.0×10^6 cells suspended in 30 µL phosphate buffered saline (PBS) orthotopically in the left lower mammary fat pad of each mouse. Experiments started when tumors reached a diameter between 6.0 and 8.0 mm (approximately 14 d after cell implantation). Animals were housed in a sterile environment and monitored daily at a temperature between 68–70 °F with a humidity of 15–20%. Lights were on for 12 hours (6 AM – 6 PM) before remaining off for the next 12 hours. Mice were randomly divided into four groups (N=4 per group) by a person blinded to the study objective and then assigned a label based on the contrast agent they would receive, namely, control (no contrast agent), barium sulfate ($BaSO_4$), Vascupaint, and Microfil.

Contrast agent preparation

$BaSO_4$ contrast was prepared by adding 5% gelatin derived from porcine skin (W/V) and 40% $BaSO_4$ to micron powder (W/V, $BaSO_4$ 97%, Thermo Fisher Scientific) into 50 mL of PBS. The solution was incubated at 37 ℃ and well shaken by hand before perfusion injection. Vascupaint contrast agent (yellow colloidal bismuth suspension MDL-121, MediLumine, Montreal, Quebec, Canada) was prepared by

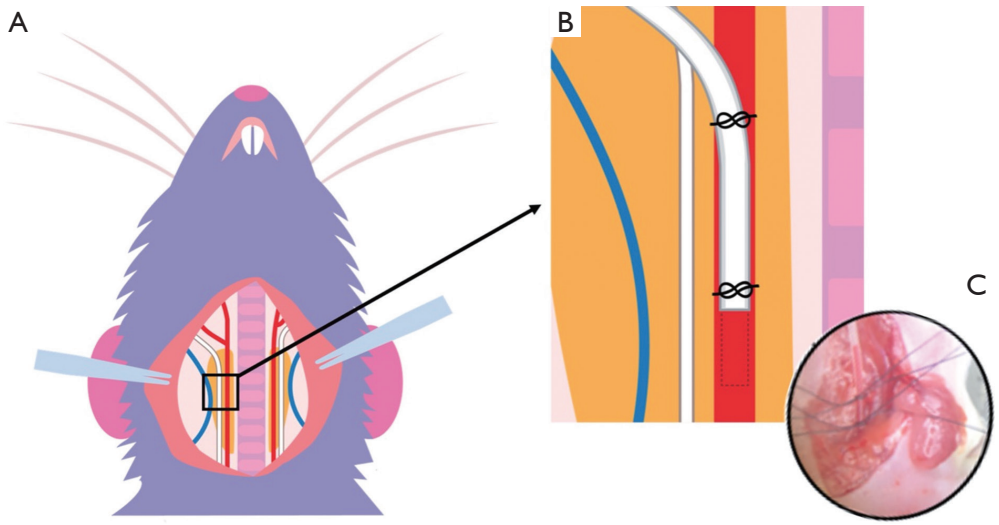

Figure 1 Transcarotid contrast agent perfusion technique. This illustration (A) highlights the transcarotid perfusion technique which isolates the carotid artery for vascular casting contrast agent perfusion and full body micro-CT imaging, where (B) represents a zoomed in view of the tubing insertion. (C) This image details this technique in a representative mouse. micro-CT, microscale computed tomography.

reducing the recommended protocol provided by mixing 1 mL of silicone agent with 1 mL diluent (MDL-121D, MediLumine) with 0.04 mL catalyst (2%, MDL-121C, MediLumine). Microfil (MV-120, Flow Tek Inc., Boulder, CO, USA) was blended by mixing 5 mL of diluent for every 4 mL of compound. The resultant mixture is catalyzed with 5% (by weight or volume) of the MV curing agent.

Transcarotid arterial perfusion

Mice were anesthetized by exposure to a combination of oxygen and 1% to 2% isoflurane and fixed in supine position. A 1 cm longitudinal skin incision was created to the midline of the neck. The carotid artery was exposed by separating fat and muscle along the right side of the trachea using forceps. Under a surgical microscope (AmScope 7X-45X Stereo Zoom microscope, United Scope LLC., Irvine, CA, USA), a 7.0 silk suture thread with two retractable knots was made from head and body sides of the artery. By gently pulling up the suture, a small arteriotomy was made between the two knots, and the tip of a PE10-polyethylene tubing (Braintree Scientific Inc., Braintree, MA, USA) was inserted at the incision point. The retractable knot at the body side was released to allow advancement of the tubing tip towards the body side. The tubing was then secured by ligatures around the artery (*Figure 1*). A syringe topped with a blunted 27G needle was inserted into the end of the catheter. Next, 2 mL of a vascular casting contrast agent (which equates to the total blood volume for a 25 g mouse) was perfused via an infusion pump at a rate of 2 mL/min. The jugular vein on the other side of the carotid artery was cut open to drain blood flow, thus allowing full perfusion of the contrast agent. This technique did not use a PBS flush nor blood removal protocol to allow the heart to perfuse the contrast agent throughout vasculature. Following complete injection of the contrast agent, the catheter was withdrawn, and the ligation was tightened. Control animals underwent the same surgical procedure but were perfused with matched doses of saline only. Successful perfusion was confirmed via visual confirmation.

Micro-CT imaging

Five minutes following successful perfusion, each animal underwent full body micro-CT imaging (OI/CT, MILabs, Utrecht, the Netherlands) after secure placement in a holder on an imaging bed. The micro-CT examination included an accurate, ultra-focus image scan at a step angle of 0.25° at 1 projection per step and a binning size of 1. The micro-CT tube settings were adjusted to a voltage of 50 kV, a current of 0.21 mA, and exposure time of 75 ms. The scanning time for a full-body and high-resolution micro-CT scans were 4 and 15 min, respectively. Approximately 30 min following full-body scans, complete brain, liver,

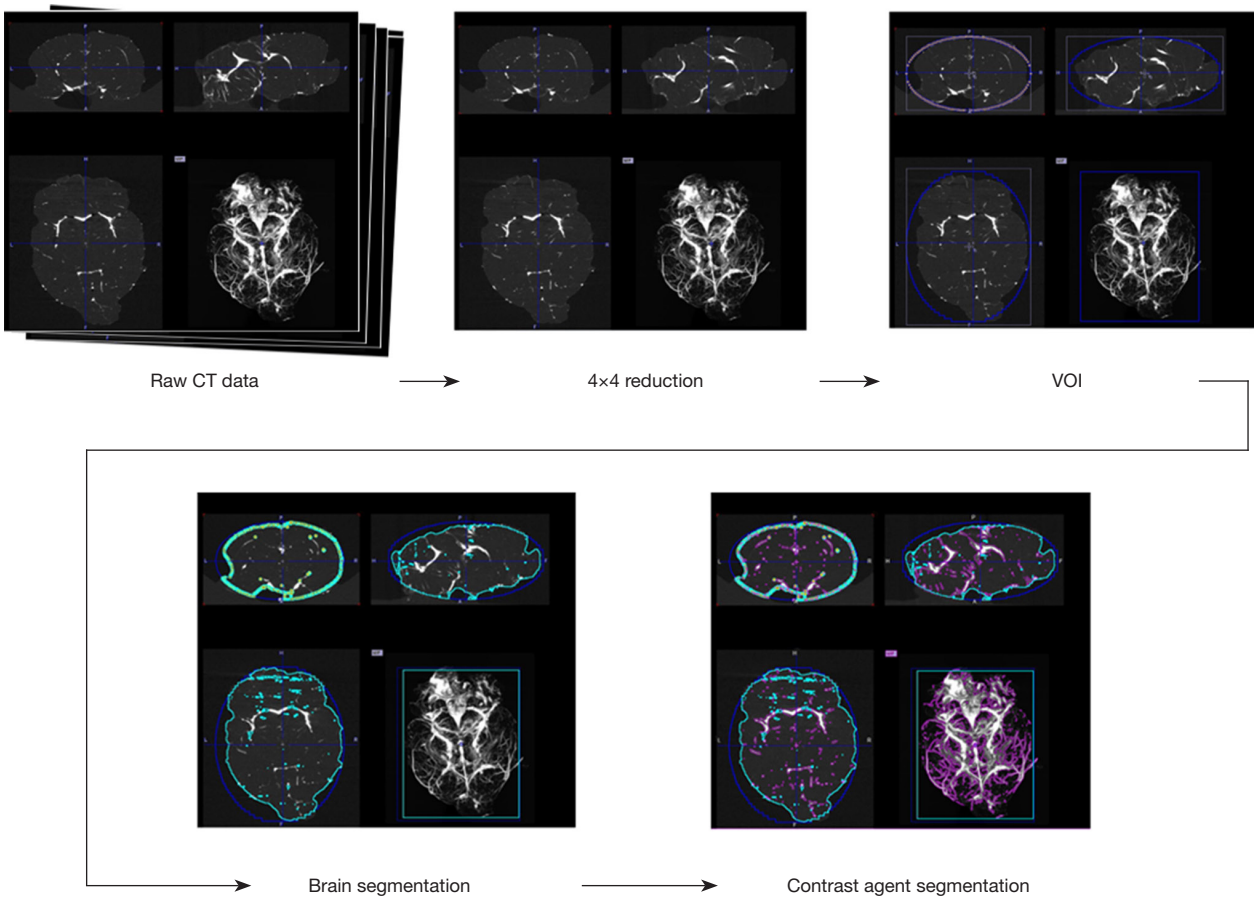

Figure 2 Schematic of post-processing workflow of micro-CT images. The post-processing analyses performed in PMOD. The raw CT images underwent a 4×4 reduction before a VOI was created around the tissue. Segmentation was performed twice to allow for highlight of contrast agent in which a mean intensity signal was calculated from. micro-CT, microscale computed tomography; VOI, volume-of-interest.

spleen, kidney, and tumor tissue were surgically removed and placed in formalin for at least 24 h before being scanned again using micro-CT and the same settings. For all scans, resolutions were selected during the post-processing stage.

Image analysis

Micro-CT images were reconstructed using vendor software and converted to Digital Imaging and Communications in Medicine (DICOM) standard files (PMOD Technologies LLC, Zurich, Switzerland) at voxel sizes of 80 and 20 µm for the full body and tissue-level scans, respectively. These were the recommended resolutions for the acquired scans. Image analysis was performed to quantify mean image intensity and the diameter of select vascular segments (*Figure 2*). Images were preprocessed by performing a 4×4 pixel-reduction, whereby each pixel matrix was averaged to produce a single pixel. This has a two-fold effect of reducing the overall computational load for subsequent processing steps while qualitatively smoothing the noise of the imaging data. Reconstructed images were quantified to extract pixel intensity information. Since the primary concern is quantifying image intensity produced by each contrast-enhanced micro-CT scan, we presumed the net reduction in image resolution has a negligible effect on this computation.

Following the reduction, a thresholding window was set to identify and remove the imaging bed. The limits of the window are set up according to the Hounsfield units (HU) corresponding to air (HU =−1,000) and bone (HU =1,000) respectively. The analytical tools within PMOD were used to set up a bounding box and volume-of-interest

(VOI) around the organ, essentially cropping the imaging bed and surrounding empty volume. The cropped image then underwent segmentation to isolate the contrast agent within each tissue type. To optimize the segmentation, a threshold relative to the soft tissue of the organ was used. Using the HU of water as reference, the threshold value was set at –100 to establish the outer boundary of the organ and to separate from the remaining empty volume not removed in prior steps. Another VOI was created using the threshold value, and the segmentation tool produced a binary preview that enabled additional processing measures, e.g., morphological closings, to perform a more robust segmentation. This feature was most applicable in instances of asymmetries and voids that create additional segmentation boundaries within the main region of the organ. Using the segmentation geometry as a VOI, the remaining area was cropped to ensure that the analysis was strictly confined to the organ. Using the statistical toolkit within PMOD, we obtained the average HU of the contrast agent per tissue type. The SNR was calculated using SNR = $(HU_{contrast} - HU_{control})/HU_{control}$, where $HU_{contrast}$ and $HU_{control}$ are the average intensities from the contrast agent and control organ, respectively. All contrast-enhanced micro-CT images were visualized using OsiriX (Pimeo, Bernex, Switzerland) with the 3D maximum intensity projection (MIP) Viewer. Images were optimized by adjusting the range of HU. Vessel diameters were measured using length tool on randomly selected slices in each animal and averaged.

Statistical analysis

A power sample analysis with an alpha of 0.05 and desired power of 0.80 was performed using preliminary data with mean image intensity values of 364.8 and 39.4 from a pilot study to determine a sample size of 4 per group. All experimental data was summarized as mean ± standard deviation. A Shapiro-Wilks test was performed to assess normality in all data. Comparisons of signal-to-noise ratio (SNR) between the different contrast-enhanced micro-CT image groups were performed using a Welch's *t*-test, while the comparison for the tumor was performed using a Mann-Whitney test. Vessel diameter measurements were evaluated using a one-way analysis of variance (ANOVA) test, with a Tukey Kramer analysis to assess differences between groups. A two-sided P value less than 0.05 was considered statistically significant. All statistical analyses were performed using Prism 9.3 (GraphPad Software Inc., San Diego, CA, USA).

Results

The primary objective of this study was to evaluate a collection of contrast agents for improved visualization of microvascular structures using *ex vivo* micro-CT imaging. These contrast agents included a barium-based solution ($BaSO_4$) and silicone rubber compound (Vascupaint) versus a gold standard vascular casting agent (Microfil MV-120). All agents were evaluated for use during contrast-enhanced micro-CT imaging of tumor-bearing mice and resultant production of optimal maps depicting vascular networks in 3D space and various tissue and organs. No tumor-bearing animals were excluded from this study and confounders were not controlled. No adverse effects occurred in the mice during this study. Experiments were deemed successful by visual confirmation of contrast agent perfusion throughout the animal body. Each animal underwent micro-CT imaging for both full body and then higher resolution tissue-level imaging after surgical excision of tumors and select organs (*Figure 3*). Collectively, these contrast-enhanced micro-CT images depict more complex vascular networks in animals perfused with Vascupaint and $BaSO_4$ compared to structures cast with Microfil.

Contrast-enhanced micro-CT images underwent quantitative analysis to calculate mean image enhancement for each tissue compared to an average signal from background tissue that had minimal or no contrast agent present. Termed the SNR, these values are summarized in *Figure 4*. In comparison to Microfil, use of both $BaSO_4$ and Vascupaint produced a significant increase in micro-CT enhancement of the brain and kidney tissue. More specifically, $BaSO_4$ had a 28- and 36-fold increase in the brain (P=0.05) and kidney (P=0.008), respectively. For comparison, Vascupaint-enhanced micro-CT image were found to have a 15- and 14-fold increase in the brain (P=0.006) and kidney (P=0.001). For the brain tissue, there was no quantitative enhancement differences in contrast-enhanced micro-CT images of the brain when using $BaSO_4$ or Vascupaint (P>0.23). However, $BaSO_4$ showed a 2.6-fold increase in the kidney over Vascupaint (P=0.03).

In general, contrast-enhanced micro-CT imaging using $BaSO_4$ and Vascupaint produced higher SNR measures in the liver and spleen than with use of Microfil. Micro-CT imaging using $BaSO_4$ produced a 3.6 and 1.8-fold image intensity increases in the liver (P=0.21) and spleen (P=0.48). Vascupaint displayed a similar trend compared to Microfil in the same organs (P>0.32). Furthermore, $BaSO_4$-enhanced micro-CT images were found to have a 1.6-fold

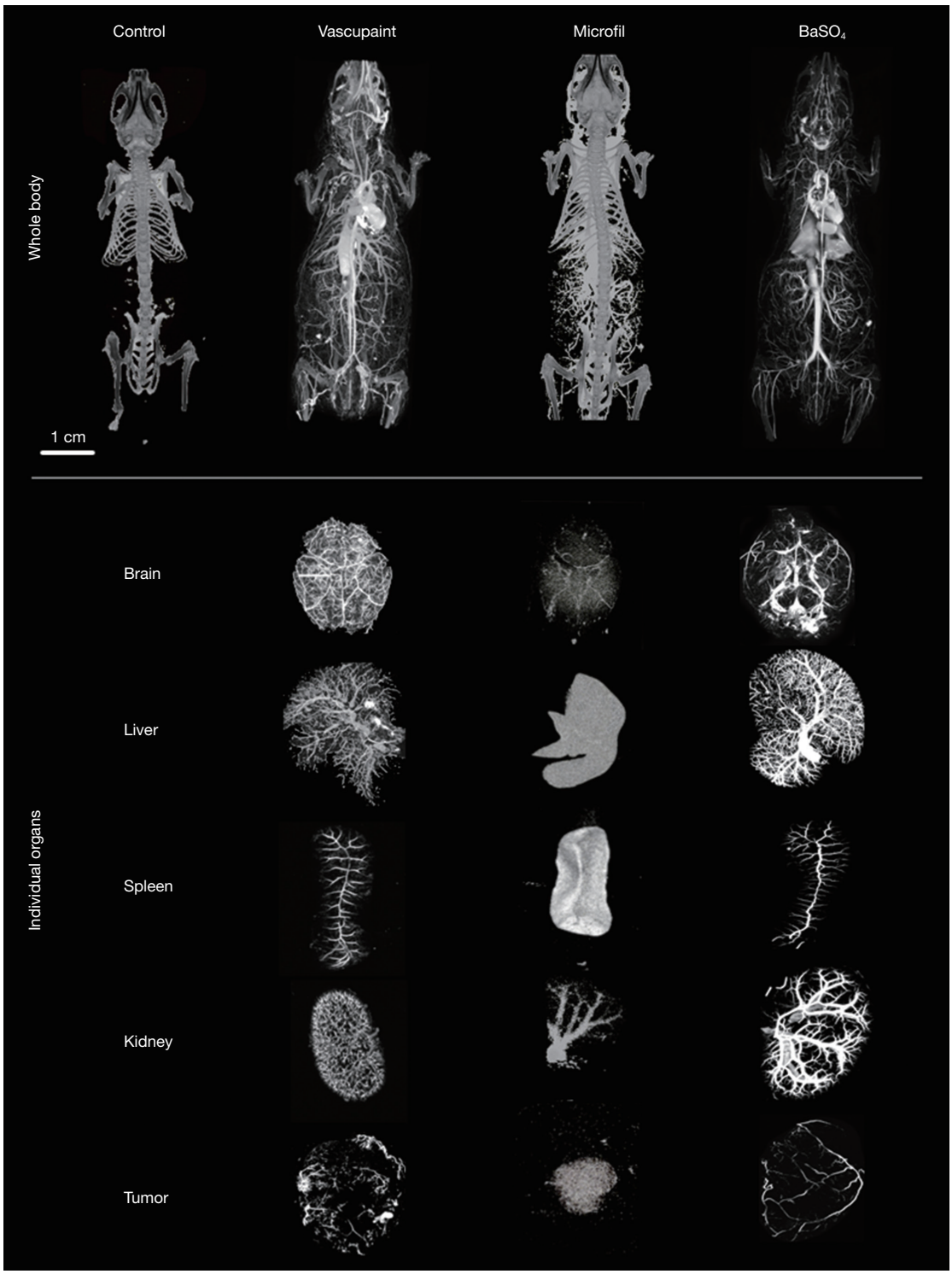

Figure 3 Qualitative comparison of contrast-enhanced micro-CT images. This figure compares whole body micro-CT images (top) and select tissues (bottom) after transcarotid perfusion of Vascupaint (left), Microfil (middle), and $BaSO_4$ (right) contrast agents. These images were scanned immediately after the perfusion and thus not enough time for the agents to harden. However, there is a noticeable difference in radiopacity between the agents. The full body images have a scale bar of 1 cm, while the specific tissues have a scale bar of 3 mm. micro-CT, microscale computed tomography; $BaSO_4$, barium sulfate.

SNR increases in the liver (P=0.49) and spleen (P=0.54) compared to Vascupaint. There was no difference between micro-CT images of the tumor vasculature for any of the contrast agents evaluated (P>0.58).

While the primary focus of this study was on achieving wholistic visualization of tumor microvasculature using contrast-enhanced micro-CT imaging, vessel diameters were measured in various tissues to determine consistency of contrast agent perfusion throughout the animal body. Specifically, image analysis software was used to measure diameter of the smallest visible vessels from randomly selected images of tumor and organs in different animals. A quantitative summary of the microvascular diameters within the tumor microenvironment are summarized in *Figure 5*, while comparison measurements from vessels found in the brain, kidney, liver, and spleen are plotted in *Figure 6*. Average vessel diameters measured from $BaSO_4$ and Vascupaint-enhanced micro-CT images were 27.5±6.1 and 24.5±2.7 μm, respectively, as compared to 90.6±15.7 μm for animals perfused with Microfil. Overall, there was no differences in the size of the smallest microvascular structures depicted in $BaSO_4$ and Vascupaint-enhanced micro-CT images of the tumor, brain, kidney, liver, or spleen (P>0.14). It was further found that use of both the $BaSO_4$ and Vascupaint contrast agents allowed visualization of much smaller vessels than that found in *ex vivo* Microfil-enhanced micro-CT images of any of the various tissue types (P<0.004).

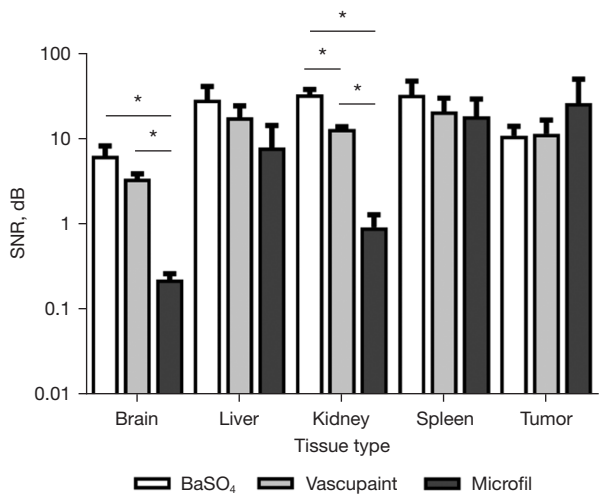

Figure 4 Quantitative summary of contrast-enhanced micro-CT images. This graph quantitatively describes the SNR measured from contrast-enhanced micro-CT images from tumor tissue and select organs. The control group (no contrast agent) was used as comparison for each group (n=4 per group). *, P<0.05. micro-CT, microscale computed tomography; SNR, signal-to-noise ratio; $BaSO_4$, barium sulfate.

Discussion

To fully understand the mechanisms behind cancer growth and metastasis, the ability to reliably visualize the entire tumor vasculature in the preclinical setting is a necessity. While several modalities have emerged, use of contrast agents and micro-CT presents the strongest argument to imaging the entire vasculature in 3D space. Moreover, micro-CT imaging allows researchers to visualize the

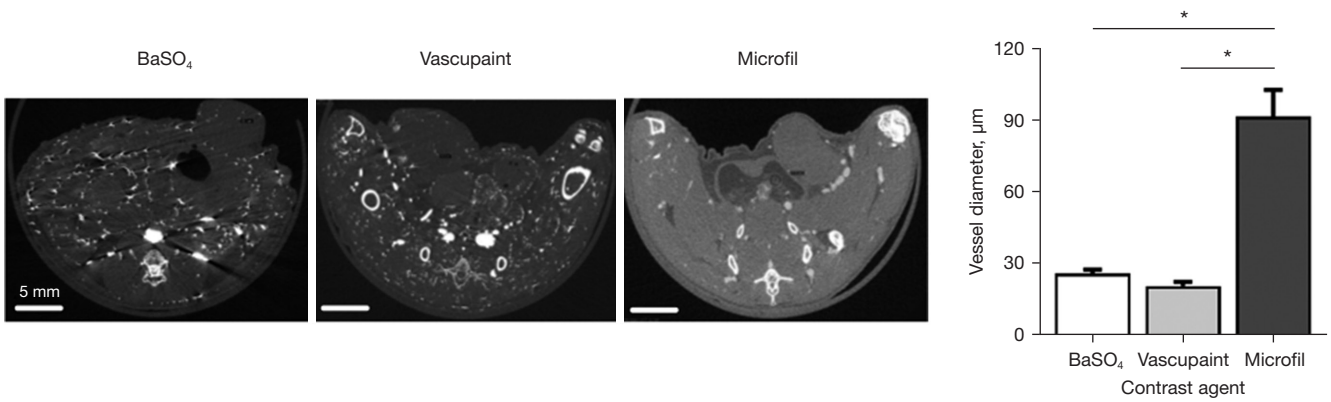

Figure 5 Summary of vessel size measurements from contrast-enhanced micro-CT images of tumor microenvironment. Representative contrast-enhanced micro-CT images of tumor tissues and a quantitative summary of all microvascular diameter measures (10 measurements per group from 4 different samples). The scale bars for the micro-CT images are 5 mm. *, P<0.05. micro-CT, microscale computed tomography; $BaSO_4$, barium sulfate.

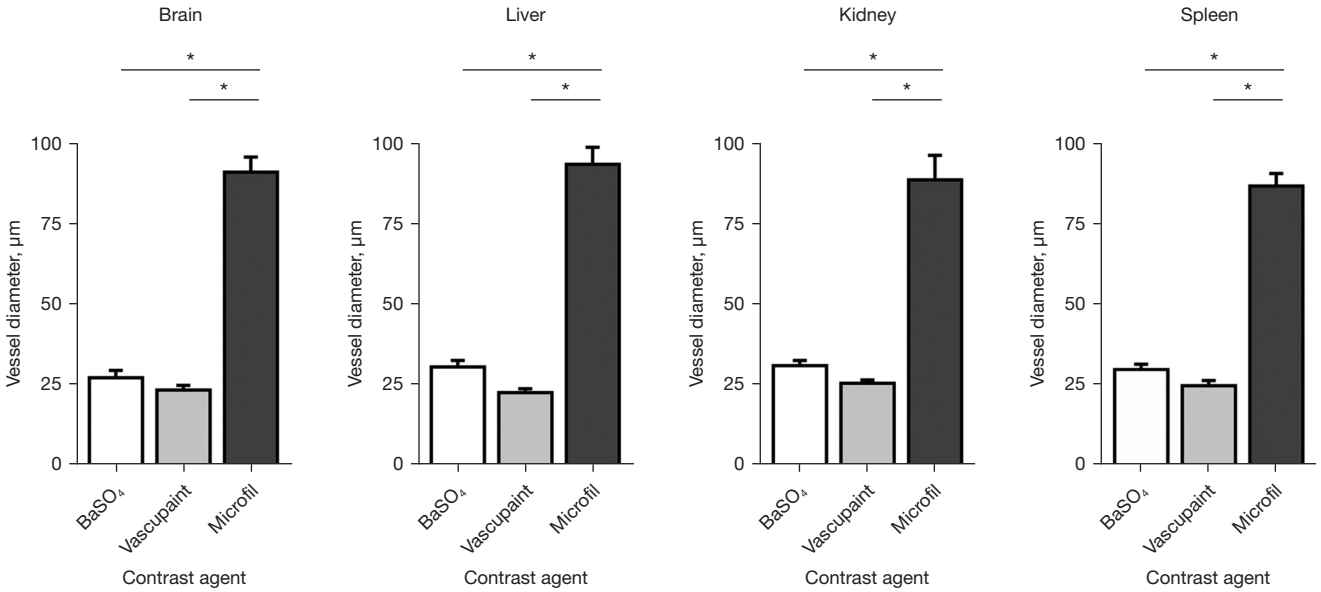

Figure 6 Summary of vessel size measurements from micro-CT images of select organs. Representative contrast-enhanced micro-CT images of the brain, kidney, liver, and spleen as well as a quantitative summary of all microvascular diameter measures (10 measurements per group from 4 different samples). *, P<0.05. micro-CT, microscale computed tomography; $BaSO_4$, barium sulfate.

microvasculature without removal of the skeletal system and depletion of the surrounding tissue typically required for casting agents. Tissue perfusion is a technique performed by many researchers who are particularly interested in understanding the microvasculature within an isolated organ like the brain to understand the central nervous system (17) or deleterious impact of stroke (10). The vasculature within the lungs has also been investigated to understand pulmonary arterial hypertension (18) or extent of cancer growth (8). Some studies have performed whole body analyses (19). Research presented herein aims to further expand the available literature by providing a comprehensive analysis of contrast-enhanced micro-CT images produced after whole body blood replacement with a commercially available colloidal bismuth suspension (Vascupaint) and a barium-based contrast agent ($BaSO_4$) in comparison to use of a polymer-based vascular casting agent (Microfil MV-120), which is commonly used for *ex vivo* tissue assessments (10). High-resolution micro-CT imaging was performed to investigate perfusion of the contrast agents throughout animal circulation by qualitative and quantitative examination of microvascular networks in tumor, brain, liver, kidney, and spleen. Our preliminary results revealed Vascupaint and $BaSO_4$-enhanced micro-CT produced superior image enhancement and microvascular visualization as compared to that found using Microfil. Notwithstanding, studies have shown Microfil-enhanced micro-CT imaging is a suitable solution for vascular enhancement throughout the full body and individual organs (19). This difference in experimental results could be attributed to the perfusion technique. Our study kept the animal alive under anesthesia during the majority of the perfusion period and utilized the heart to naturally pump the contrast agent throughout the vasculature. Meanwhile, blood was drained via the jugular vein allowing for a compete replacement of blood pool by the contrast agent. The 2 mL perfusion volume of contrast agent is based on the fact that the total blood volume for a 25 g mouse is about 2 mL. Other perfusion techniques completely remove the blood and rinse with PBS before manually injecting the contrast agent in dead animals. These techniques perfuse through a cardiac puncture, which can produce insufficient blood pool filling due to contrast agent leakage into the chest cavity. This frequently leads to poorer images or even complete experimental failure. Another study was performed comparing the various perfusion techniques and effect on visualization of the microvascular network in lung cancer (18). These results showed that some techniques lead to either inconsistent filling or overfilling of the tumor vasculature.

Vascularization within tumors (or other organs) is usually quantified using microvessel density via histology or visual count of blood vessels (8). However, both are subjective processes and not indicative of the entire sample. Additionally, there is sectioning bias associated with histology that can misrepresent a tortuous vessel as several on a single slice. For this study, assessment of contrast-enhanced micro-CT imaging using various contrast agents was evaluated by SNR values and vessel diameter size measurements, which are common metrics (9,18,19). Using cancer-bearing mice, our research demonstrated that Vascupaint and $BaSO_4$-enhanced micro-CT images of both the whole body as well as excised tumors and organs were superior to Microfil, which was attributed to more complete filling of smaller microvascular segments and consistent with previous studies (20). However, SNR can be misleading metric. Microfil has a lower radiopacity than the barium contrast agent (10) and Vascupaint, which results in a lower SNR. While our qualitative images supported a more detailed vascular visualization, more methods are needed to quantitatively compare vascular casting agents. One study used machine learning to analyze the 3D vascular network to extract parameters such as volume fraction, mean vessel diameter, and vascular volume (21). Moreover, these results are a product of the image processing used in this study. High-resolution scans were post-processed at 20 µm and then underwent a 4×4 pixel-reduction. Both values were performed due to limitations with our processing computer. Ultimately, images should have been post-processed at a 4 µm voxel size resolution and no pixel reduction, but our computer was unable to handle larger files. Furthermore, even with the limitations of histological analyses, vascular staining should be performed in future experiments to compare quantitative information with micro-CT images.

Another study compared brain cerebrovascular structures following $BaSO_4$ and Microfil filling (10). Both contrast agents both demonstrated uniform perfusion. However, unlike the $BaSO_4$ used in our study, the barium used by Hong *et al.* was the product of $BaCl_2$ and $MgSO_4$. This is because the commercially available barium powder showed higher micro-CT image enhancement albeit nonuniform. Our study confirmed these results. Furthermore, Hong *et al.* showed that the barium was unable to perfuse through the arterial vessels. Further analysis would need to be performed to determine whether barium is capable of perfusing through the lungs in future experiments.

Despite the benefits of CT imaging in combination with contrast agents, it is primarily used in a preclinical setting. Researchers concerned with temporal studies use *in vivo* contrast agents as vascular casting contrast agents are terminal studies. *In vivo* contrast agents have also been shown to linger in animals. Fenestra LC was still visible within the liver and spleen tissue more than 20 d post-injection (14) while Exitron nano 6,000 and 12,000 were shown to be visible in liver tissue more than 150 d post-injection (22). With these agents, researchers aim to achieve high spatial resolutions, so longer micro-CT scan times are required (5). In addition, post processing required to analyze tissue microvasculature is a demanding process. These limitations are overcome using vascular casting contrast agents as these agents produce increased enhancement of vasculature following micro-CT imaging. Since this technique is not clinically relevant, researchers have investigated the use of contrast agents with ultrasound to visualize vasculature. To that end, super-resolution ultrasound (SRUS) similarly uses contrast agents to visualize microvascular structures (23,24). This method relies on the detection and localization of individual microbubble contrast agents in the image planes, allowing unprecedented spatial resolution on a scale of tens of micrometers and at clinically relevant penetration depths (25). The current limitation with the SRUS technique is the need of an independent modality to help validate image reconstruction and processing algorithms. Most contrast-enhanced ultrasound imaging studies have relied on vascular flow phantoms for *in vitro* validation (26,27). Therefore, there is an opportunity for contrast-enhanced micro-CT imaging to be used for *in vivo* experimental validation. One study compared these two methods in rat brain microvasculature (28). This study demonstrated that both contrast-enhanced micro-CT and SRUS imaging produced similar results with minimal differences. Tissue vasculature was slightly modified in the micro-CT images due to the extraction and fixation of the brain, but high-resolution angiography provided superior microvascular enhancement.

Conclusions

Tissue perfusion with vascular casting contrast agents followed by micro-CT imaging provides the optimal technique for visualization of microvascular networks in 3D space. Our research suggests that Vascupaint and $BaSO_4$-enhanced micro-CT images are superior to those produced using the vascular casting agent Microfil agent. Given our experimental protocol and assuming Vascupaint and $BaSO_4$ allowed more complete tissue perfusion, contrast-enhanced

micro-CT using these two different agents allowed visualization of much smaller microvascular structures compared to studies using Microfil. Notwithstanding, there were noted inconsistencies between results suggesting selection of contrast agent for any micro-CT study should be carefully considered and based on tissue of interest as well as perfusion technique.

Acknowledgments

We would like to acknowledge Dr. Girgis Obaid for his contributions in experimental design and administrative support.
Funding: This research was supported in part by the National Institutes of Health (NIH) grants (Nos. R01CA269973, R01DK126833, R01EB025841, and R21EB034441); and an award from the Cancer Prevention and Research Institute of Texas (CPRIT) to establish the Small Animal Imaging Facility at the University of Texas at Dallas (No. RP180670).

Footnote

Reporting Checklist: The authors have completed the ARRIVE reporting checklist. Available at https://qims.amegroups.com/article/view/10.21037/qims-23-901/rc

Conflicts of Interest: All authors have completed the ICMJE uniform disclosure form (available at https://qims.amegroups.com/article/view/10.21037/qims-23-901/coif). The authors have no conflicts of interest to declare.

Ethical Statement: The authors are accountable for all aspects of the work in ensuring that the questions related to the accuracy or integrity of any part of the work are appropriately investigated and resolved. This study was approved by the Institutional Ethics Committee of the University of Texas at Dallas in compliance with national guidelines for the care and use of animals (OLAW Assurance Number: A3329-01 and USDA License Number: 74-R-0066).

References

1. Kleinsmith LJ. Principles of cancer biology. San Francisco: Pearson Benjamin Cummings; 2006:312.
2. DeVita VT, Lawrence TS, Rosenberg SA, editors. Cancer: principles & practice of oncology. Primer of the molecular biology of cancer. Third edition. Philadelphia: Wolters Kluwer; 2021.
3. Sweeney MD, Kisler K, Montagne A, Toga AW, Zlokovic BV. The role of brain vasculature in neurodegenerative disorders. Nat Neurosci 2018;21:1318-31.
4. Schaad L, Hlushchuk R, Barré S, Gianni-Barrera R, Haberthür D, Banfi A, Djonov V. Correlative Imaging of the Murine Hind Limb Vasculature and Muscle Tissue by MicroCT and Light Microscopy. Sci Rep 2017;7:41842.
5. Ghaghada KB, Badea CT, Karumbaiah L, Fettig N, Bellamkonda RV, Johnson GA, Annapragada A. Evaluation of tumor microenvironment in an animal model using a nanoparticle contrast agent in computed tomography imaging. Acad Radiol 2011;18:20-30.
6. Siegel RL, Miller KD, Wagle NS, Jemal A. Cancer statistics, 2023. CA Cancer J Clin 2023;73:17-48.
7. Lindsay TH, Jonas BM, Sevcik MA, Kubota K, Halvorson KG, Ghilardi JR, Kuskowski MA, Stelow EB, Mukherjee P, Gendler SJ, Wong GY, Mantyh PW. Pancreatic cancer pain and its correlation with changes in tumor vasculature, macrophage infiltration, neuronal innervation, body weight and disease progression. Pain 2005;119:233-46.
8. Savai R, Langheinrich AC, Schermuly RT, Pullamsetti SS, Dumitrascu R, Traupe H, Rau WS, Seeger W, Grimminger F, Banat GA. Evaluation of angiogenesis using micro-computed tomography in a xenograft mouse model of lung cancer. Neoplasia 2009;11:48-56.
9. Folarin AA, Konerding MA, Timonen J, Nagl S, Pedley RB. Three-dimensional analysis of tumour vascular corrosion casts using stereoimaging and micro-computed tomography. Microvasc Res 2010;80:89-98.
10. Hong SH, Herman AM, Stephenson JM, Wu T, Bahadur AN, Burns AR, Marrelli SP, Wythe JD. Development of barium-based low viscosity contrast agents for micro CT vascular casting: Application to 3D visualization of the adult mouse cerebrovasculature. J Neurosci Res 2020;98:312-24.
11. Minnich B, Lametschwandtner A. Lengths measurements

in microvascular corrosion castings: two-dimensional versus three-dimensional morphometry. Scanning 2000;22:173-7.
12. Hainfeld JF, Ridwan SM, Stanishevskiy Y, Smilowitz NR, Davis J, Smilowitz HM. Small, Long Blood Half-Life Iodine Nanoparticle for Vascular and Tumor Imaging. Sci Rep 2018;8:13803.
13. Renard Y, Hossu G, Chen B, Krebs M, Labrousse M, Perez M. A guide for effective anatomical vascularization studies: useful ex vivo methods for both CT and MRI imaging before dissection. J Anat 2018;232:15-25.
14. Boll H, Figueiredo G, Fiebig T, Nittka S, Doyon F, Kerl HU, Nölte I, Förster A, Kramer M, Brockmann MA. Comparison of Fenestra LC, ExiTron nano 6000, and ExiTron nano 12000 for micro-CT imaging of liver and spleen in mice. Acad Radiol 2013;20:1137-43.
15. de Bournonville S, Vangrunderbeeck S, Kerckhofs G. Contrast-Enhanced MicroCT for Virtual 3D Anatomical Pathology of Biological Tissues: A Literature Review. Contrast Media Mol Imaging 2019;2019:8617406.
16. Kuo W, Schulz G, Müller B, Kurtcuoglu V. Evaluation of metal nanoparticle- and plastic resin-based x-ray contrast agents for kidney capillary imaging. SPIE Opt Eng Appl 2019;11113:137-49.
17. Hlushchuk R, Haberthür D, Soukup P, Barré SF, Khoma OZ, Schittny J, Haghayegh Jahromi N, Bouchet A, Engelhardt B, Djonov V. Innovative high-resolution microCT imaging of animal brain vasculature. Brain Struct Funct 2020;225:2885-95.
18. Deng Y, Rowe KJ, Chaudhary KR, Yang A, Mei SHJ, Stewart DJ. Optimizing imaging of the rat pulmonary microvasculature by micro-computed tomography. Pulm Circ 2019;9:2045894019883613.
19. Vasquez SX, Gao F, Su F, Grijalva V, Pope J, Martin B, Stinstra J, Masner M, Shah N, Weinstein DM, Farias-Eisner R, Reddy ST. Optimization of microCT imaging and blood vessel diameter quantitation of preclinical specimen vasculature with radiopaque polymer injection medium. PLoS One 2011;6:e19099.
20. Ghanavati S, Yu LX, Lerch JP, Sled JG. A perfusion procedure for imaging of the mouse cerebral vasculature by X-ray micro-CT. J Neurosci Methods 2014;221:70-7.
21. Kostrikov S, Johnsen KB, Braunstein TH, Gudbergsson JM, Fliedner FP, Obara EAA, Hamerlik P, Hansen AE, Kjaer A, Hempel C, Andresen TL. Optical tissue clearing and machine learning can precisely characterize extravasation and blood vessel architecture in brain tumors. Commun Biol 2021;4:815.
22. Boll H, Nittka S, Doyon F, Neumaier M, Marx A, Kramer M, Groden C, Brockmann MA. Micro-CT based experimental liver imaging using a nanoparticulate contrast agent: a longitudinal study in mice. PLoS One 2011;6:e25692.
23. Ghosh D, Xiong F, Sirsi SR, Shaul PW, Mattrey RF, Hoyt K. Toward optimization of in vivo super-resolution ultrasound imaging using size-selected microbubble contrast agents. Med Phys 2017;44:6304-13.
24. Ghosh D, Peng J, Brown K, Sirsi S, Mineo C, Shaul PW, Hoyt K. Super-Resolution Ultrasound Imaging of Skeletal Muscle Microvascular Dysfunction in an Animal Model of Type 2 Diabetes. J Ultrasound Med 2019;38:2589-99.
25. Brown KG, Li J, Margolis R, Trinh B, Eisenbrey JR, Hoyt K. Assessment of Transarterial Chemoembolization Using Super-resolution Ultrasound Imaging and a Rat Model of Hepatocellular Carcinoma. Ultrasound Med Biol 2023;49:1318-26.
26. Brown KG, Ghosh D, Hoyt K. Deep Learning of Spatiotemporal Filtering for Fast Super-Resolution Ultrasound Imaging. IEEE Trans Ultrason Ferroelectr Freq Control 2020;67:1820-9.
27. Özdemir İ, Johnson K, Mohr-Allen S, Peak KE, Varner V, Hoyt K. Three-dimensional visualization and improved quantification with super-resolution ultrasound imaging - validation framework for analysis of microvascular morphology using a chicken embryo model. Phys Med Biol 2021;66:10.1088/1361-6560/abf203.
28. Chavignon A, Heiles B, Hingot V, Orset C, Vivien D, Couture O. 3D Transcranial Ultrasound Localization Microscopy in the Rat Brain With a Multiplexed Matrix Probe. IEEE Trans Biomed Eng 2022;69:2132-42.

Cite this article as: Margolis R, Merlo B, Chanthavisay D, Chavez C, Trinh B, Li J. Comparison of micro-CT image enhancement after use of different vascular casting agents. Quant Imaging Med Surg 2024;14(3):2568-2579. doi: 10.21037/qims-23-901

